

Quantifying non-stabilizerness efficiently via information scrambling

Arash Ahmadi* and Eliska Greplova

Kavli Institute of Nanoscience, Delft University of Technology, Delft, the Netherlands

The advent of quantum technologies brought forward much attention to the theoretical characterization of the computational resources they provide. A method to quantify quantum resources is to use a class of functions called magic monotones, which are, however, notoriously hard and impractical to evaluate for large system sizes. In recent studies, a fundamental connection between information scrambling and magic monotones was established. This connection simplified magic monotone calculation, but this class of methods still suffers from the exponential scaling with respect to the number of qubits. In this work, we establish an efficient way to sample an out-of-time-order correlator that approximate magic monotones. We numerically show the relation of these sampled correlators to different non-stabilizerness measures for both qubit and qutrit systems. Furthermore, we put forward and simulate a protocol to measure the monotonic behaviour of magic for the time evolution of local Hamiltonians.

I. INTRODUCTION

The field of quantum computing introduced the concept that quantum systems can deliver a significant computational speed-up in a variety of settings [1–6]. Yet, although increasingly large quantum processors are available, the question remains of how to rigorously quantify the computational resources of a quantum computer. One successful approach towards determining quantum resources of a quantum state is to calculate how “far away” the state is from being possible to simulate efficiently with a classical computer [7].

A specific example of quantum states that are tractable to represent and simulate on a classical computer are the so-called stabilizer states [8]. These states result from quantum circuits produced by Clifford gates which are elements of the Clifford group generated by the Hadamard gate, the phase gate and the entangling control-NOT gate [9]. In order to get any quantum advantage over classical computers, we need to add additional gates outside of the Clifford group. By injecting more non-Clifford gates into a quantum circuit, we obtain a quantum state with further distance from a stabilizer state. This distance is in literature referred to as magic or non-stabilizerness [10]. The states that are not stabilizer states are called *magic states*. Interestingly, in the context of quantum error correction, the Clifford gates can be implemented fault-tolerantly [11, 12], while universal gate-sets are achieved by the distillation of a large number of noisy magic states into a less-noisy magic state which subsequently provides the computational resources for the fault-tolerant quantum computation [7, 13–16]

Examples of magic monotones include magical cross-entropy, mana [10], and robustness of magic [14]. These measures are, however, computationally expensive to evaluate and their calculation requires exact knowledge of the wave-function combined with complex optimization [10], which excludes the study of large quantum cir-

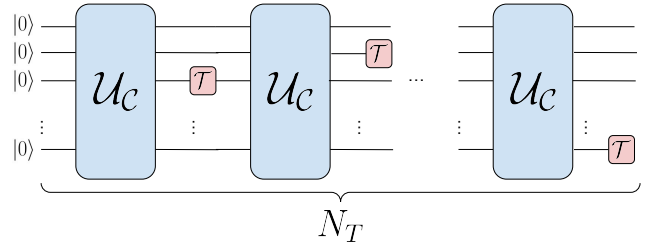


Figure 1. The schematic structure of a t-doped quantum circuit. We are using a block of the random Clifford gates, \mathcal{U}_C followed by a T-gate on a random qudit. We repeat this process N_T times.

cuits. More recently introduced magic monotones such as the Gottesman-Kitaev-Preskill magic measure and the stabilizer Renyi entropy, [17, 18], offer simplified scaling which enables exact calculation of magic for approximately up to 12 qubits using conventional computers.

Different approaches to describe how far a quantum state is from the stabilizer state, can also be related to the amount of quantum correlations in the system. The out-of-time ordered correlators (OTOCs) quantify quantum information scrambling [19–24]. Quantum information scrambling describes the spread of the local information in a quantum system [23]. Through the time evolution of a closed quantum system, the information about initial state of the system can become very hard to access due to quantum correlations in the system [25]. Even though the information is still encoded in the system it is not directly accessible without measuring all its degrees of freedom. Information scrambling has recently attracted an increasing amount of attention due to the relation with the anti-de Sitter/conformal field theory (AdS/CFT) correspondence [26]. The AdS/CFT correspondence draws a duality that relates the noise in quantum error correction codes to information scrambling in black holes [19, 21, 22]. Another application of this concept emerged in condensed matter physics such as many-body localization [27] and non-Fermi liquid behaviours [28].

* a.ahmadi-1@tudelft.nl

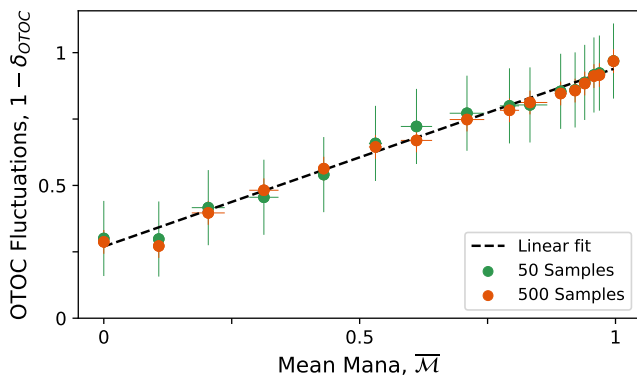


Figure 2. The fluctuation of OTOC, $1 - \delta_{OTOC}$ as a function of the mean value of mana, $\overline{\mathcal{M}}$. We see a linear behaviour between these two magic monotones for 6 qutrit t-doped circuits. Here we show results for 50 (green dots) and 500 (orange dots) random samples of OTOC on the y-axis. On the x-axis, we calculated mana for 10 of the samples and we fit a linear dependence (dashed line). The vertical error bar is the statistical error calculated as the inverse of the square root of the number of samples and the horizontal error bar corresponds to the standard deviation of mana.

Moreover, it was recently experimentally demonstrated that OTOCs can be used as an indicator of the degree of non-stabilizerness of scrambled quantum circuits [29]. In parallel, recent work has shown an analytical relation between the non-stabilizerness and OTOC [18, 30].

In this work, we show the relation between a randomised sampling of OTOC fluctuations and mana for qutrit systems and stabiliser Renyi entropy for qubit systems. We show numerical evidence that this method requires dramatically lesser number of OTOC measurements in comparison to the exact methods of calculating magic monotones. Capitalizing on this relation, we put forward an experimentally feasible way to approximate magic using the evaluation of OTOCs. Our work lays foundation to approximate magic in a scalable way in larger systems, as our protocol is designed to be adaptable for both numerical techniques such as tensor networks [31] and neural networks [32] as well as experimental measurements [29].

II. METHODS

A. Magic

The concept of magic in quantum information science arises from the field of resource theory [33]. The Gottesman-Knill theorem [8] guarantees that the subset of the physical states known as *stabilizer* states are efficiently simulatable on a classical computer. More precisely, the stabilizer states are the second level of the Clifford hierarchy [9].

Since the first level (the Pauli gates) and the second

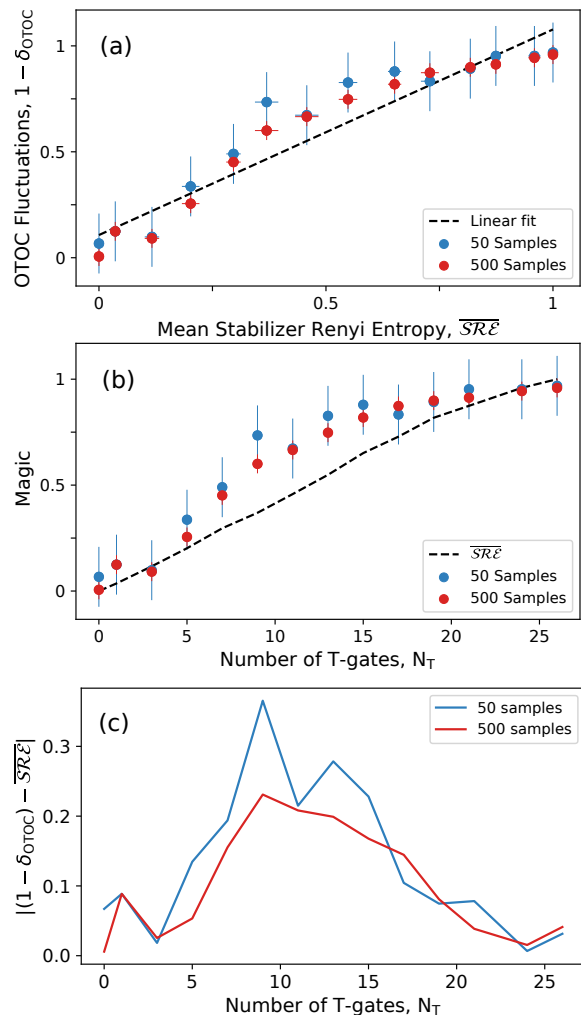


Figure 3. a. The fluctuation of OTOC, $1 - \delta_{OTOC}$ over 50 (blue dots) and 500 (red dots) samples as a function of the mean value of stabiliser Renyi entropy (dashed line), $\overline{\mathcal{SRE}}$ over 10 samples. The vertical error bar is the statistical error (the inverse of the square root of the number of samples) and the horizontal error represents the standard deviation of $\overline{\mathcal{SRE}}$. b. The comparison of the exact values of the $\overline{\mathcal{SRE}}$ with the approximated values $1 - \delta_{OTOC}$ for 50 and 500 samples as a function of the number of T-gates in the circuit, N_T . c. The absolute error of approximated and exact magic, $|(1 - \delta_{OTOC}) - \overline{\mathcal{SRE}}|$, as a function of the number of T-gates in the circuit, N_T . The blue line represents the error for 50 samples, and the red line represents the error for 500 samples.

level, (the Clifford gates) of the Clifford hierarchy are insufficient for universal quantum computing, we need to use the third-level gates. This level of Clifford's hierarchy includes, for example, a T-gate. Another set of important non-Clifford gates are the rotation gates $\{R_x(\theta), R_y(\theta), R_z(\theta)\}$, where θ is the angle of rotation. These gates are particularly important in problems that require a continuous set of parameters to tune, i.e. quantum machine learning algorithms [5, 6].

The amount of non-stabilizerness, or magic, of any state is measured using *magic monotones*. Magic monotones such as the robustness of magic [10] are based on an optimization over all stabilizer states, which make them practically hard to compute. However, one example of a magic monotone that does not require any optimization is known as mana, \mathcal{M} [10]. This magic monotone has another limitation, namely that it is only definable for odd-prime dimensional Hilbert spaces. Additionally, mana is practically very hard to calculate since it is based on calculating discrete Wigner functions which in practice limits current calculations to at most 6 qudits. More details regarding the definition and evaluation of mana are available in Appendix A.

Another magic monotone introduced for qubits is the Stabilizer Renyi Entropy [18]. For a system of N qubits, the Stabilizer Renyi Entropy of order n is defined as

$$M_n(|\Psi_N\rangle) = (1 - n)^{-1} \log \sum_{P \in \mathcal{P}_N} \frac{\langle \Psi_N | P | \Psi_N \rangle^{2n}}{2^N}, \quad (1)$$

where \mathcal{P}_N is the set of all N -qubit Pauli strings and the number of the Pauli strings in \mathcal{P}_N we are summing over scales as 4^N .

B. Information scrambling

A well-known measure of information scrambling is the out-of-time-order correlators (OTOCs) which are commonly used in high-energy physics and condensed matter physics [19–24, 27, 28]. OTOC is evaluated for any two operators W and V as

$$OTOC(t) = \text{Re}(\langle W^\dagger(t) V^\dagger W(t) V \rangle), \quad (2)$$

where

$$W(t) = U^\dagger(t) W(0) U(t), \quad (3)$$

and $U(t)$ is the time evolution operator, which could either result from time evolution of a Hamiltonian or from a quantum circuit. Here we will consider a N qudit system and we take $W(0) = X_{N-1}$ and $V = Z_1$ where X_i and Z_i are the conventional Pauli operators and the subscript indicates the i -th qudit. In this case, $W(0)$ plays the role of the butterfly operator in studying chaotic quantum systems. The reason for using the butterfly operator is that by including a small perturbation (in this case a bit flip) we are disturbing the reversibility of the system, which is a signature of chaos [34]. The information scrambling measured through OTOC describes how information spreads in the system and becomes inaccessible in later times [19–24]. Information scrambling also describes how local Heisenberg operators grow in time [29, 35, 36]. A way to assess how the OTOC value fluctuates over a set of random circuits is the OTOC fluctuation, δ_{OTOC} , defined as the standard deviation of OTOC over all measured instances of OTOC.

III. RESULTS

A. Mana and OTOC

We will now numerically investigate the relation between the fluctuations of OTOC, which was experimentally observed in Ref. [29] to decrease with the growing non-stabilizerness of the quantum circuit, and the measure for quantum complexity, mana, \mathcal{M} for $q = 3$ and the stabilizer Renyi entropy, M_2 for $q = 2$. To this end, we design random quantum circuits with Clifford and non-Clifford gates, known as t-doped quantum circuits. First, we consider N qudits in q -dimensional Hilbert space where $q = 3$. The circuits consist of M cycles of Clifford gates. In each cycle, we first apply one single Clifford gate, randomly chosen from the set $\mathcal{S} = \{H, S, X, Y, Z, I\}$ on each qudit. Then we add two CSUM gates on two randomly chosen qudits, where the CSUM gate is the counterpart of CNOT in Hilbert spaces with $q > 2$. Here we have a fixed number of $M = 10$ random cycles for each block of random Cliffords. Finally, we add a single non-Clifford gate, T , on a randomly chosen qudit. We increase the magic in the circuit by increasing the number of layers of the random Cliffords followed by a T-gate.

We begin by analyzing the relationship of mana and OTOC in the Hilbert space of dimension $q = 3$ for circuits containing four qutrits such that mana is well-defined and computationally tractable. We use the qutrit Clifford gates introduced in [37]. We provide detailed definitions of all gates in Appendix B.

We observe a decreasing monotonous relation between the mean value of mana, $\bar{\mathcal{M}}$ and the OTOC fluctuations, δ_{OTOC} , see Fig. 2. Note that mana is an extensive function [38]; hence we normalize it with respect to the local Hilbert space dimension, q and the number of qudits, N . The upper bound for mana of the Haar random state has been shown to be $\frac{1}{2}(N \log q - \log \pi/2)$ [39]. This normalization is performed for ease of comparison between different methods of magic determination. In Fig. 2, we observe a linear dependence between $1 - \delta_{OTOC}$ and $\bar{\mathcal{M}}$. This relationship corresponds to the linear fit $1 - \delta_{OTOC} = 0.67\bar{\mathcal{M}} + 0.27$. We simulated the OTOC instances of 50 and 500 circuit runs and the number of T-gates in the circuit is $N_T \in [0, 20]$. We note that the linear dependence is independent of the number of samples used in this example while a smaller number of samples naturally leads to larger statistical error in estimating δ_{OTOC} . For the simulation of the quantum circuits, we have used the Cirq package [40].

B. The Stabilizer Renyi entropy and OTOC

Mana, discussed in the previous section, is not only challenging from the scaling point of view but also only defined for odd-dimensional local Hilbert space and thus not possible to evaluate for qubits. In this section, we

compare OTOC fluctuations, δ_{OTOC} , with the stabilizer Renyi entropy, M_2 , which is well-defined for even-dimensional Hilbert spaces. To evaluate the stabilizer Renyi entropy we use Eq. (1) for $q = 2$ and $n = 2$. The authors of Ref. [18] have shown the relation of the stabilizer Renyi entropy with 8-OTOC. The main difference between our approach with the existing analytical formula in Ref. [18] is the random sampling of a constant number of OTOCs as opposed to the exponential scaling of the number of 8-OTOC terms in the Renyi entropy formula [18].

We use the same random circuits as described in the previous section (see Fig. 1), this time for qubits. This way we obtain a comparison between δ_{OTOC} and the exact stabilizer Renyi entropy. We also note that since the δ_{OTOC} range is between 0 and 1, we will normalize the \overline{SRE} with respect to its saturation value. In Fig. 3a, we show OTOC fluctuations as a function of mean Renyi entropy, \overline{SRE} and find a dependence corresponding to the fit $1 - \delta_{OTOC} = 0.97\overline{SRE} + 0.10$. Moreover, in Fig. 3b we show amount of magic in the circuit as a function of number of T-gates, N_T , calculated using two different methods: the exact stabilizer Renyi entropy (dashed line) and the OTOC fluctuation, $1 - \delta_{OTOC}$, method. For OTOC fluctuations, we show again instances of averaging over 50 samples, and averaging over 500 samples in order to exemplify the independence of the sampling size as well as the corresponding statistical error bars. The circuits used for Fig. 3a and b are 12 qubit t-doped circuits and we calculate \overline{SRE} from 10 random instances. Each point in Fig. 3a belongs to a certain number of T-gates in the circuit, $N_T \in [0, 26]$ as seen in Fig. 3b. We note that the range of N_T was motivated by the fact that it has been shown that we need more than or equal to $2N$ T-gates to saturate the magic [41]. We see that regardless of the number of T-gates (and hence the amount of magic in the circuit), our ability to approximate the stabilizer Renyi entropy using OTOC fluctuations remains similar. Increasing the number of samples by an order of magnitude shows minor improvement due to the smaller amount of statistical errors. We quantify this improvement in Fig. 3c where we show the absolute error between the normalized mean of stabilizer Renyi entropy and approximated magic via OTOC sampling. The notable observation is that the absolute error for both sample counts is higher in the intermediate region of the T-gate count.

Since OTOC fluctuations is the numerically lesser demanding method to estimate magic, we expand the previously achieved upper bound in literature and estimate the magic for 14 qubit T-doped circuits. This system size appears to be beyond the power of the previously introduced methods non-stabilizerness evaluation methods due to the combination of large demands of the full set of Pauli strings and increased circuit simulation complexity for a larger number of qubits. The results obtained with OTOC-sampling methods introduced here are shown in fig. 4. We used T-doped circuits with 14 qubits and sampled 50 OTOC instances where circuits

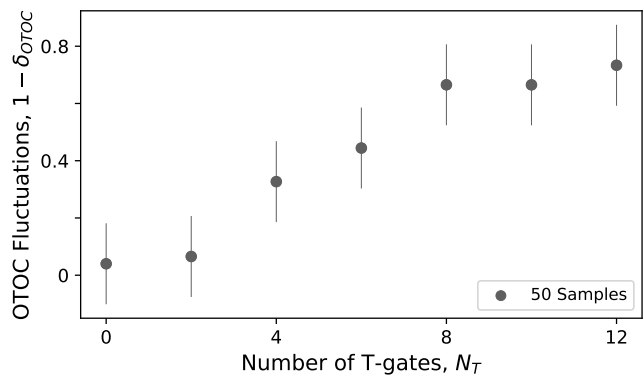


Figure 4. The approximated magic for 14 qubit T-doped random circuits with fluctuations of OTOC, $1 - \delta_{OTOC}$ as a function of the number of T-gates in the system, N_T , for 50 samples of OTOC.

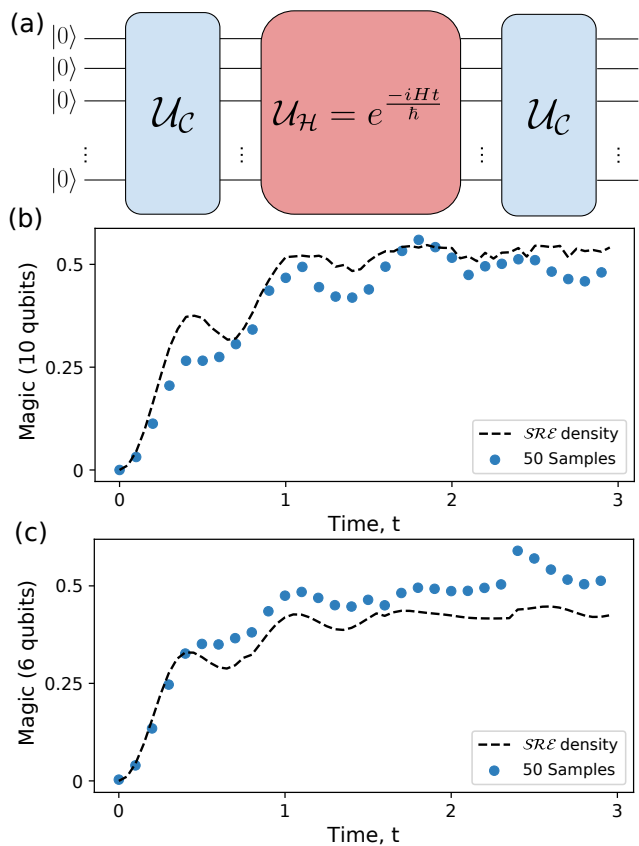


Figure 5. a. The schematic structure of measuring magic of a time evolution of the Hamiltonian, \mathcal{U}_H . The protocol consists of two random Clifford blocks, before and after the desired time evolution block. b. The comparison of OTOC fluctuations (blue dots) with the exact stabilizer Renyi entropy density (dashed line). The simulation is done for 10 qubits. c. The comparison of OTOC fluctuations (blue dots) with the exact stabilizer Renyi entropy density (dashed line) for 6 qubit system.

contain $N_T \in [0, 12]$ T-gates.

C. The magic generated by time evolution of a Hamiltonian

In this section, we propose a protocol to measure the magic generated by time evolution under the general Hamiltonian. The time evolution unitary operator of a general time-independent Hamiltonian is a fixed operator. In order to create diversity in measured instances of OTOC we need to introduce randomisation in the circuit. We achieve this goal by including two extra blocks of random Clifford circuits, one before the time evolution and one after, see Fig. 5a. Since Clifford gates do not produce any magic by definition, we do not lose any generality for the circuit's magic calculation. It is important to keep in mind that the depth of the random Clifford circuit needs to be sufficient to fully scramble the state.

Here as an example, we consider the Hamiltonian of the transverse-field Ising Hamiltonian,

$$H = -J \sum_i Z_i Z_{i+1} - h \sum_i X_i, \quad (4)$$

The system is in the open boundary condition where Z and X are the Pauli matrices. For this simulation, we fix $J = 1$ and $h = 0.5$. The schematic structure of the circuit we consider for its time evolution is shown in Fig. 5.

We want to emphasise that the results in this section are not normalized, unlike the t-doped circuits in sections A and III B. The reason is that we do not have an upper bound for magic, unlike Haar states. We already know that magic density is an extensive property [38], but the OTOC fluctuation possesses numbers between 0 and 1. So for a different number of qubits, we expect the exact magic density values to change but the OTOC fluctuations do not. The key thing is the overall monotonic behaviour remains the same. From Fig. 5b we can see that the density of SRE for the local Hamiltonian of the Eq. 4 and OTOC fluctuations show similar behaviour. In this simulation, we used 10 qubits with 50 instances of sampled OTOCs. The time evolves for a total time of $3/J$. We see the same trend of increment in magic in the early time and oscillatory behaviour and stabilization in both stabilizer Renyi entropy density and approximated OTOC fluctuations. We expect that the scale of the density of magic changes with the number of qubits while OTOC fluctuations stay the same and the overall behaviour of both be similar. In Fig. 5c we can observe a similar behaviour of fluctuations of OTOC with respect to time while the scale of the stabilizer Renyi entropy density is changed to 6 qubits but the trend and monotonicity of the magic behaviour is the same. We used the Qiskit package [42] for this simulation.

IV. CONCLUSION AND DISCUSSION

We have shown aspects of the relation between mana and random sampling of OTOC fluctuations for t-doped circuits which were previously unexplored. In addition to that, we provided numerical evidence that OTOC fluctuation sampling in the scrambled circuits is a scalable measure for magic. We were able to mirror scaling and behavior for stabilizer Renyi entropy and for mana with significantly lower number measurements.

Although the limiting behaviours of OTOC fluctuations (the zero magic and the saturated magic) have been studied before [43, 44], the intermediate regime was previously unexplored and we addressed this gap numerically in this work. We see that the accuracy of sampled OTOC approximation is lower in this regime. The underlying reasons for this behavior constitute an open question for further work and possible connections to the chaoticity of the time evolution might be explored [41].

Ref. [30] put forward a statement that the fluctuations of OTOC are always smaller or equal to a specific type of magic monotone. In this work, we complement this statement by numerically showing the relation of OTOC fluctuations to the stabilizer Renyi entropy. We analyzed the accuracy of stabilizer Renyi entropy approximation as a function of the number of samples drawn from scrambled random circuits. While the majority of our simulated data points fulfil the inequality derived in Ref. [30], it is not always the case. This observation is an interesting starting point for further investigation.

Additionally, we also extended the method of sampling scrambling random circuits to approximate magic to Hamiltonian evolution and numerically calculated magic for time evolution governed by Ising Hamiltonian in a transverse field with very good results in comparison with stabilizer Renyi entropy.

A key aspect of the magic approximation method we proposed in this paper is its scalability. Our simulations show that for 12 qubit system how the measurement of as little as 50 OTOC instances can very well approximate the exact magic measurement that would require around 16×10^6 8-OTOC or Pauli string measurements [18]. While our work does not provide analytical convergence guarantees, all the available numerical evidence suggests that our protocol can work as a powerful numerically and experimentally inexpensive sampling method for estimating magic. For the system sizes studied in this work, we have not encountered any evidence that the sampling complexity should be exponential in the number of qubits which we exemplified this statement by approximating magic and showing its monotonicity in a 14-qubit t-doped system. Such 14-qubit systems are currently not accessible for evaluation with other measures we successfully approximated in this work.

Interesting research direction going forward is to combine our sampling approach with experiment [29] or approximate numerical methods such as tensor networks [31, 45] and neural networks [32]. Our method can be

used alongside, or as a complement to other existing approximation methods [46–48].

All code required to reproduce results presented in this manuscript is available at [49].

Appendix A: Mana

One of the magic monotones is known as *mana*. The restriction of mana is that it is only well-defined for odd prime-dimensional Hilbert spaces. Here, we introduce it for q -dim Hilbert spaces [10] with q an odd prime number. To show how to calculate mana, we first need to define the clock and shift operators corresponding to the q -dimensional Pauli Z gate and Pauli X gate [37],

$$Z = \sum_{n=0}^{q-1} \omega^n |n\rangle \langle n|, \quad X = \sum_{n=0}^{q-1} |n+1 \bmod q\rangle \langle n| \quad (\text{A1})$$

with $\omega = e^{2\pi i/q}$. The other necessary definition is the Heisenberg-Weyl operators in prime dimensions,

$$T_{aa'} = \omega^{-2^{-1}aa'} Z^a X^{a'} \quad (\text{A2})$$

where $2^{-1} = \frac{q+1}{2}$ (the multiplicative inverse of 2 mod q) and $(a, a') \in \mathbb{Z}_q \times \mathbb{Z}_q$. By following this definition, we can define Pauli strings as

$$T_{\mathbf{a}} = T_{a_1 a'_1} \otimes T_{a_2 a'_2} \dots \otimes T_{a_N a'_N}. \quad (\text{A3})$$

Now, we can define a new basis set for the Hilbert space, known as phase space point operators,

$$A_{\mathbf{b}} = q^{-N} T_{\mathbf{b}} \left[\sum_{\mathbf{a}} T_{\mathbf{a}} \right] T_{\mathbf{b}}^\dagger \quad (\text{A4})$$

and these phase space point operators form a complete basis set for $\mathbb{C}^{q^N \otimes q^N}$. Thus, we can expand any density matrix ρ in this basis,

$$\rho = \sum_{\mathbf{u}} W_{\rho}(\mathbf{u}) A_{\mathbf{u}} \quad (\text{A5})$$

The coefficients $W_{\rho}(\mathbf{u})$ are called discrete Wigner functions and we can define mana as

$$\mathcal{M}(\rho) = \log \sum_{\mathbf{u}} |W_{\rho}(\mathbf{u})| \quad (\text{A6})$$

As we already stated in the main text, we are dealing with Clifford and non-Clifford operations. The Clifford gates map Pauli strings to other Pauli strings, up to an arbitrary phase [38],

$$C = \{U : UT_{\mathbf{a}}U^\dagger = e^{i\phi} T_{\mathbf{b}}\}. \quad (\text{A7})$$

Since the Clifford gates map each of these Pauli strings to each other, each Clifford unitaries also map the computational basis to one of the eigenstates of Pauli strings. These eigenstates are called stabilizer states. Since stabilizer states are prepared with only Clifford gates, their mana is *zero*.

Appendix B: Clifford and non-Clifford gates definitions

In this appendix we are introducing the gates that we have used in this study. We introduce both for 2-dimensional Hilbert spaces and higher dimensional Hilbert spaces.

1. Clifford gates

The set of Clifford gates is the second level of Clifford hierarchy [9] that are the following gates in 2-dimensional Hilbert spaces,

$$H_2 = \frac{1}{\sqrt{2}} \begin{bmatrix} 1 & 1 \\ 1 & -1 \end{bmatrix}, \quad P_2 = \begin{bmatrix} 1 & 0 \\ 0 & i \end{bmatrix} \quad (\text{B1})$$

$$\text{CNOT} = |0\rangle \langle 0| \otimes I + |1\rangle \langle 1| \otimes X$$

The generalization of these gates is straightforward [50]. The d -dimensional Hadamard gate, H_d , is

$$H_d |j\rangle = \frac{1}{\sqrt{d}} \sum_{i=0}^{d-1} \omega^{ij} |i\rangle \quad j \in \{0, 1, 2, \dots, d-1\} \quad (\text{B2})$$

where $\omega := e^{2\pi i/d}$. The next gate is the d -dimensional Phase gate, P_d ,

$$P_d |j\rangle = \omega^{j(j-1)/2} |j\rangle \quad (\text{B3})$$

and, finally, the generalized CNOT gate that is known as $CSUM_d$ gate and defined as

$$CSUM_d |i, j\rangle = |i, i+j \pmod{d}\rangle \quad i, j \in \{0, 1, 2, \dots, d-1\} \quad (\text{B4})$$

2. Non-Clifford gates

Clifford gates are not sufficient for universal quantum computation and we at least need one non-Clifford gate to have this universality [51, 52]. One of these gate is the T-gate that emerges from the third level Clifford hierarchy. The definition of T-gate for 2-dimensional Hilbert space is

$$T_2 = \begin{bmatrix} 1 & 0 \\ 0 & e^{i\pi/4} \end{bmatrix} \quad (\text{B5})$$

The generalization of T-gate to higher dimensional Hilbert spaces is not so straightforward [37]. Here, we only write down the matrices of the T-gate for 3-dimensional Hilbert spaces which are useful for us. The 3-dimensional Hilbert space T-gate is

$$T_3 = \begin{bmatrix} 1 & 0 & 0 \\ 0 & e^{2\pi i/9} & 0 \\ 0 & 0 & e^{-2\pi i/9} \end{bmatrix}, \quad (\text{B6})$$

-
- [1] Peter W. Shor. Polynomial-time algorithms for prime factorization and discrete logarithms on a quantum computer. *SIAM Review*, 41(2):303–332, 1999.
- [2] Lov K. Grover. A fast quantum mechanical algorithm for database search, 1996.
- [3] Scott Aaronson and Alex Arkhipov. The computational complexity of linear optics. *Theory of Computing*, 9(4):143–252, 2013.
- [4] Yudong Cao, Jonathan Romero, Jonathan P. Olson, Matthias Degroote, Peter D. Johnson, Mária Kieferová, Ian D. Kivlichan, Tim Menke, Borja Peropadre, Nicolas P. D. Sawaya, Sukin Sim, Libor Veis, and Alán Aspuru-Guzik. Quantum chemistry in the age of quantum computing. *Chemical Reviews*, 119(19):10856–10915, 2019. PMID: 31469277.
- [5] Abhinav Kandala, Antonio Mezzacapo, Kristan Temme, Maika Takita, Markus Brink, Jerry M. Chow, and Jay M. Gambetta. Hardware-efficient variational quantum eigensolver for small molecules and quantum magnets. *Nature*, 549(7671):242–246, Sep 2017.
- [6] Edward Farhi, Jeffrey Goldstone, and Sam Gutmann. A quantum approximate optimization algorithm, 2014.
- [7] Sergey Bravyi and Alexei Kitaev. Universal quantum computation with ideal clifford gates and noisy ancillas. *Phys. Rev. A*, 71:022316, Feb 2005.
- [8] Daniel Gottesman. The heisenberg representation of quantum computers. 1998.
- [9] Daniel Gottesman and Isaac L. Chuang. Demonstrating the viability of universal quantum computation using teleportation and single-qubit operations. *Nature*, 402(6760):390–393, 1999.
- [10] Victor Veitch, S A Hamed Mousavian, Daniel Gottesman, and Joseph Emerson. The resource theory of stabilizer quantum computation. *New Journal of Physics*, 16(1):013009, 2014.
- [11] Daniel Gottesman. Theory of fault-tolerant quantum computation. *Physical Review A*, 57(1):127–137, jan 1998.
- [12] Peter W. Shor. Fault-tolerant quantum computation, 1996.
- [13] Michael Beverland, Earl Campbell, Mark Howard, and Vadym Kliuchnikov. Lower bounds on the non-clifford resources for quantum computations. *Quantum Science and Technology*, 5(3):035009, may 2020.
- [14] Mark Howard and Earl Campbell. Application of a resource theory for magic states to fault-tolerant quantum computing. *Physical Review Letters*, 118(9), mar 2017.
- [15] Earl T Campbell and Joe O’Gorman. An efficient magic state approach to small angle rotations. *Quantum Science and Technology*, 1(1):015007, dec 2016.
- [16] Earl T. Campbell. Catalysis and activation of magic states in fault-tolerant architectures. *Physical Review A*, 83(3), mar 2011.
- [17] Oliver Hahn, Alessandro Ferraro, Lina Hultquist, Giulia Ferrini, and Laura Garcí a-Álvarez. Quantifying qubit magic resource with gottesman-kitaev-preskill encoding. *Physical Review Letters*, 128(21), may 2022.
- [18] Lorenzo Leone, Salvatore F. E. Oliviero, and Alioscia Hamma. Stabilizer rényi entropy. *Physical Review Letters*, 128(5), feb 2022.
- [19] Patrick Hayden and John Preskill. Black holes as mirrors: quantum information in random subsystems. *Journal of High Energy Physics*, 2007(09):120–120, Sep 2007.
- [20] Yasuhiro Sekino and L Susskind. Fast scramblers. *Journal of High Energy Physics*, 2008(10):065–065, oct 2008.
- [21] Stephen H. Shenker and Douglas Stanford. Black holes and the butterfly effect. *Journal of High Energy Physics*, 2014(3):67, March 2014.
- [22] Juan Maldacena, Stephen H. Shenker, and Douglas Stanford. A bound on chaos. *Journal of High Energy Physics*, 2016(8), Aug 2016.
- [23] Pavan Hosur, Xiao-Liang Qi, Daniel A. Roberts, and Beni Yoshida. Chaos in quantum channels. *Journal of High Energy Physics*, 2016(2), Feb 2016.
- [24] Daniel A. Roberts and Beni Yoshida. Chaos and complexity by design. *Journal of High Energy Physics*, 2017(4), apr 2017.
- [25] Yongliang Zhang. Information scrambling in quantum many-body systems. *Dissertation (Ph.D.)*, Feb 2020.
- [26] Ahmed Almheiri, Xi Dong, and Daniel Harlow. Bulk locality and quantum error correction in ads/cft. *Journal of High Energy Physics*, 2015(4), 2015.
- [27] D.M. Basko, I.L. Aleiner, and B.L. Altshuler. Metal-insulator transition in a weakly interacting many-electron system with localized single-particle states. *Annals of Physics*, 321(5):1126–1205, May 2006.
- [28] Daniel Ben-Zion and John McGreevy. Strange metal from local quantum chaos. *Physical Review B*, 97(15), Apr 2018.
- [29] Xiao Mi, Pedram Roushan, Chris Quintana, Salvatore Mandrà, Jeffrey Marshall, Charles Neill, Frank Arute, Kunal Arya, Juan Atalaya, Ryan Babbush, and et al. Information scrambling in quantum circuits. *Science*, 374(6574):1479–1483, Dec 2021.
- [30] Roy J. Garcia, Kaifeng Bu, and Arthur Jaffe. Resource theory of quantum scrambling. *Proceedings of the National Academy of Sciences*, 120(17):e2217031120, 2023.
- [31] Shenglong Xu and Brian Swingle. Scrambling dynamics and out-of-time ordered correlators in quantum many-body systems: a tutorial, 2022.
- [32] Yukai Wu, L.-M. Duan, and Dong-Ling Deng. Artificial neural network based computation for out-of-time-ordered correlators. *Physical Review B*, 101(21), jun 2020.
- [33] Eric Chitambar and Gilad Gour. Quantum resource theories. *Reviews of Modern Physics*, 91(2), Apr 2019.
- [34] Xiao Chen, Rahul M. Nandkishore, and Andrew Lucas. Quantum butterfly effect in polarized floquet systems. *Physical Review B*, 101(6), feb 2020.
- [35] Xiao-Liang Qi and Alexandre Streicher. Quantum epidemiology: operator growth, thermal effects, and SYK. *Journal of High Energy Physics*, 2019(8), aug 2019.
- [36] Daniel E. Parker, Xiangyu Cao, Alexander Avdoshkin, Thomas Scaffidi, and Ehud Altman. A universal operator growth hypothesis. *Physical Review X*, 9(4), oct 2019.
- [37] Yuchen Wang, Zixuan Hu, Barry C. Sanders, and Sabre Kais. Qudits and high-dimensional quantum computing. *Frontiers in Physics*, 8, 2020.
- [38] Christopher David White, Chunjun Cao, and Brian Swingle. Conformal field theories are magical. *Physical Review B*, 103(7), 2021.
- [39] Christopher David White and Justin H. Wilson. Mana

- in haar-random states, 2020.
- [40] Cirq Developers. Cirq, August 2021. See full list of authors on Github: <https://github.com/quantumlib/Cirq/graphs/contributors>.
- [41] Lorenzo Leone, Salvatore F. E. Oliviero, You Zhou, and Alioscia Hamma. Quantum Chaos is Quantum. *Quantum*, 5:453, May 2021.
- [42] MD SAJID ANIS, Abby-Mitchell, Héctor Abraham, AduOffei, Rochisha Agarwal, Gabriele Agliardi, Merav Aharoni, Ismail Yunus Akhalwaya, and et al. Qiskit: An open-source framework for quantum computing, 2021.
- [43] Vitali D. Milman and Gideon Schechtman. *Asymptotic Theory of Finite Dimensional Normed Spaces*. Springer, Heidelberg, 1986.
- [44] Emiliano M. Fortes, Ignacio Garcí a-Mata, Rodolfo A. Jalabert, and Diego A. Wisniacki. Gauging classical and quantum integrability through out-of-time-ordered correlators. *Physical Review E*, 100(4), oct 2019.
- [45] Tobias Haug and Lorenzo Piroli. Quantifying nonstabilizerness of matrix product states. *Physical Review B*, 107(3), jan 2023.
- [46] Tobias Haug and M.S. Kim. Scalable measures of magic resource for quantum computers. *PRX Quantum*, 4(1), jan 2023.
- [47] Tobias Haug, Soovin Lee, and M. S. Kim. Efficient stabilizer entropies for quantum computers, 2023.
- [48] Poetri Sonya Tarabunga, Emanuele Tirrito, Titas Chanda, and Marcello Dalmonte. Many-body magic via pauli-markov chains – from criticality to gauge theories, 2023.
- [49] Arash Ahmadi and Eliska Greplova. Magic Info Scrambling. <https://gitlab.com/QMAI/papers/magicinfoscrumbling>.
- [50] Daniel Gottesman. Fault-tolerant quantum computation with higher-dimensional systems. *Chaos, Solitons & Fractals*, 10(10):1749–1758, Sep 1999.
- [51] Adriano Barenco, Charles H. Bennett, Richard Cleve, David P. DiVincenzo, Norman Margolus, Peter Shor, Tycho Sleator, John A. Smolin, and Harald Weinfurter. Elementary gates for quantum computation. *Physical Review A*, 52(5):3457–3467, nov 1995.
- [52] P.Oscar Boykin, Tal Mor, Matthew Pulver, Vwani Roychowdhury, and Farrokh Vatan. A new universal and fault-tolerant quantum basis. *Information Processing Letters*, 75(3):101–107, 2000.